Available online at www.sciencedirect.com

ScienceDirect

Ceramics International 40 (2014) 1525–1529

CERAMICS INTERNATIONAL

www.elsevier.com/locate/ceramint

Methane oxidation behavior over $La_{0.08}Sr_{0.92}Fe_{0.20}Ti_{0.80}O_{3-\delta}$ perovskite oxide for SOFC anode

Jong Seol Yoon[a], Eun Jeong Yi[a], Byung Hyun Choi[b], Mi-Jung Ji[b], Hae Jin Hwang[a,*]

[a]*Division of Materials Science and Engineering, Inha University, 253 Yonghyun-dong, Nam-gu, Incheon 402-751, Republic of Korea*

[b]*Optic and Electronic Ceramics Division, Korea Institute of Ceramic Engineering and Technology, 233-5 Gasan-dong, Geumcheon-gu, Seoul 153-801, Republic of Korea*

Received 10 June 2013; received in revised form 8 July 2013; accepted 8 July 2013
Available online 16 July 2013

Abstract

A single phase perovskite-type $La_{0.08}Sr_{0.92}Fe_{0.20}Ti_{0.80}O_{3-\delta}$ catalyst was fabricated in air at 800 °C using the Pechini method. The methane conversion rate and hydrogen selectivity over the $La_{0.08}Sr_{0.92}Fe_{0.20}Ti_{0.80}O_{3-\delta}$ catalyst were evaluated over the temperature range, 300–900 °C. Complete and partial methane oxidation were predominant at the low and high temperature regions, respectively. The complete oxidation of methane was attributed to a suprafacial mechanism. On the other hand, an intrafacial mechanism might be responsible for the partial oxidation of methane at high temperatures. XPS showed that Fe ions were active sites for methane oxidation reactions over the $La_{0.08}Sr_{0.92}Fe_{0.20}Ti_{0.80}O_{3-\delta}$ catalyst. The methane conversion rate and hydrogen selectivity at 900 °C were 52% and 66%, respectively.

Keywords: D. Perovskite; Oxide anode; Doped-$SrTiO_3$; Methane oxidation; Catalytic activity

1. Introduction

Solid oxide fuel cells (SOFCs) are energy conversion devices that can convert the chemical energy of fuels, such as hydrogen or hydrocarbons, to electrical energy directly [1]. Recently, there has been increasing interest in developing oxide anode materials as an alternative to a traditional Ni–YSZ cermet to allow the use of hydrocarbons as the fuels because the Ni–YSZ cermet anode suffers from long-term performance degradation caused by carbon deposition [2–5].

To overcome this problem, oxide anodes are considered as alternative SOFC anode materials. Among the possible oxide anode materials, perovskite-type doped $SrTiO_3$ are most promising because of its good phase stability and high electronic conductivity under a reducing atmosphere. In particular, many studies have reported La doped $SrTiO_3$ to be a likely anode material for SOFCs because of its high electrical conductivity under a reduced atmosphere [6–8]. On the other hand, La-doped $SrTiO_3$ shows poor catalytic activity for hydrogen oxidation reactions under normal SOFC operating temperatures. Therefore, by partially replacing titanium with transition metals, such as iron, cobalt, etc., the catalytic activity can be improved as a result of the production of oxygen vacancies and the altered oxidation state of the transition metals. In this study, 8 mol% La and 20 mol% Fe co-doped $SrTiO_3$ perovskite was prepared using the Pechini method. The methane oxidation behavior was evaluated using a fixed-bed reactor system as a function of temperature. In addition, X-ray photoelectron spectroscopy (XPS) was used to identify the active site for the methane oxidation reaction.

2. Experimental procedure

2.1. Powder preparation

The La and Fe co-doped perovskite-type $La_{0.08}Sr_{0.92}Fe_{0.20}Ti_{0.80}O_{3-\delta}$ powder was synthesized using the Pechini method. Fig. 1 shows a flow chart for the powder synthesis method. Strontium nitrate (98.0%, Aldrich), lanthanum nitrate (99.0%, Aldrich), titanium isopropoxide (97.0%, Aldrich), iron nitrate

*Corresponding author. Tel.: +82 32 860 7521; fax: +82 32 862 4482.
E-mail address: hjhwang@inha.ac.kr (H.J. Hwang).

0272-8842/$ - see front matter © 2013 Elsevier Ltd and Techna Group S.r.l. All rights reserved.
http://dx.doi.org/10.1016/j.ceramint.2013.07.038

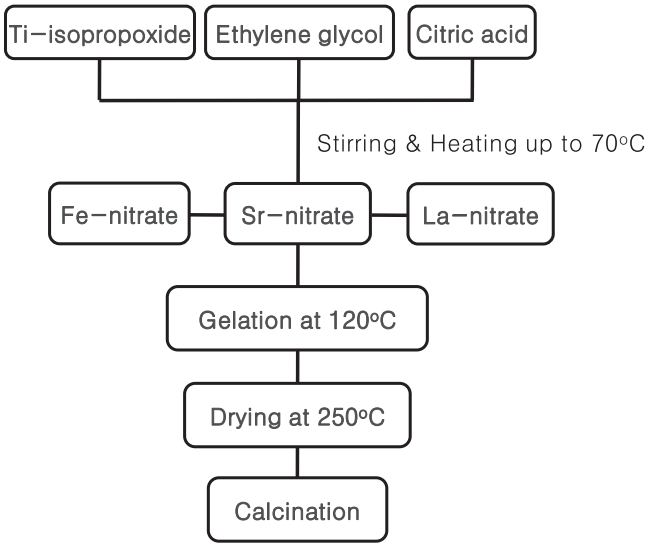

Fig. 1. Flow chart for catalyst powder synthesis.

(99.9%, Aldrich), citric acid (99.5%, Junsei) and ethylene glycol (99.5%, Junsei) were used as starting materials. The molar ratio of metal nitrates, citric acid and ethylene glycol was 1:2:8. An appropriate amount of titanium isopropoxide was dissolved in ethylene glycol. Citric acid and the other metal nitrates were then added sequentially. The entire process was carried out in a glove box in a deactivated nitrogen gas atmosphere to avoid moisture contact. When the solution was heated to 80 °C, a polyesterification reaction occurred between ethylene glycol and citric acid. The solution was further heated to 120 °C for 8 h to remove the water produced by polyesterification. During heating at 120 °C, the solution transformed to a viscous polymeric resin. The resin was dried at 250 °C for 12 h and the perovskite powder was obtained by calcining the resin at 800 °C for 5 h.

2.2. TG/DTA characterizations

To examine the decomposition behavior of the precursor resins, the dried resins were loaded in an alumina crucible and examined by thermogravimetric (TG)/differential thermal analysis (DTA; STA 409 PC, Netzsch). The samples were heated to 1000 °C at the rate of 10 °C/min.

2.3. XPS surface analysis

The surface structure of the perovskite catalyst was examined by X-ray photoelectron spectroscopy (XPS). The XPS curves were referenced to the C 1s value of 285.0 eV, which is due to atmospheric contamination and is always present on a solid surface [9]. Curve fitting was conducted using the standard Gaussian–Lorentzian deconvolution method.

2.4. Catalytic activity evaluation

The catalytic activity for methane oxidation was measured using a fixed-bed quartz reactor (inner diameter: 18 mm, length: 760 mm) under steady state conditions at atmospheric pressure. Fig. 2 shows the experimental setup for the methane oxidation test. The catalyst powder (100 mg) was diluted with quartz sand (50–70 mesh, 1 g) to avoid sintering between the catalyst particles at the high operating temperature. The diluted catalyst samples were inserted into the middle of the quartz tube between quartz wools. The total feed flow rate was 50 SCCM (mixture containing 2% O_2 and 4% CH_4—balanced by Ar) and was controlled by mass flow controllers (Horiba STEC co., Ltd.). The flow rate of each reactant gas was controlled by mass flow controllers. Methane conversion was measured at 300–900 °C. The reactor was equilibrated for 30 min at each temperature before the measurement. The molar concentrations of the product gases were analyzed by on-line micro gas chromatography (CP-4900, Varian).

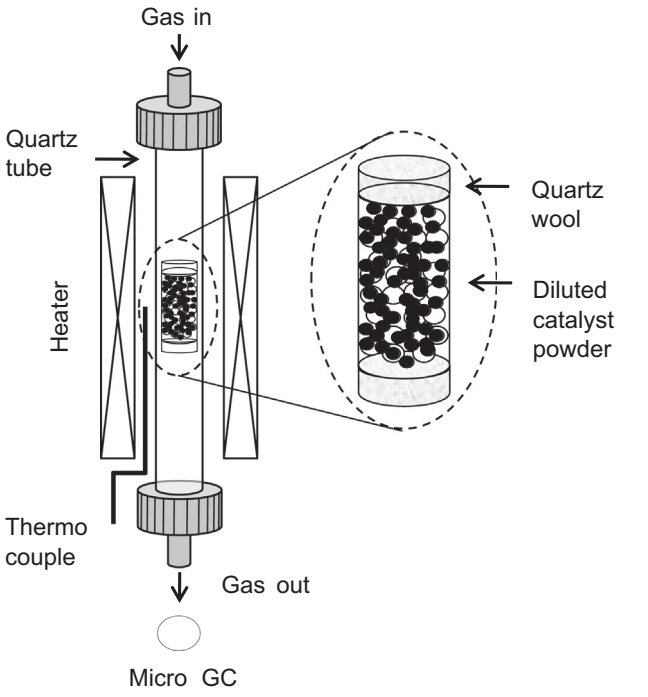

Fig. 2. Schematic diagram of the fixed-bed quartz reactor for evaluating the methane oxidation behavior.

3. Results

TG/DTA analysis was carried out to examine the thermal behavior of the polymeric precursor (Fig. 3). Decomposition occurred in three steps before obtaining the perovskite-type $La_{0.08}Sr_{0.92}Fe_{0.20}Ti_{0.80}O_{3-\delta}$ oxide. The TG curve showed three weight losses. The first weight loss between 100 °C and 200 °C was assigned to the dehydration and evaporation of the residual ethylene glycol. The second weight loss between 280 °C and 550 °C was associated with the decomposition and burnout of the organic components. The third slight weight loss above 550 °C was attributed to decomposition of the oxycarbonate intermediates or residual carbonates [10,11]. The DTA curve displays some modest exothermic peaks at 350–460 °C, as well as a significant exothermic peak at

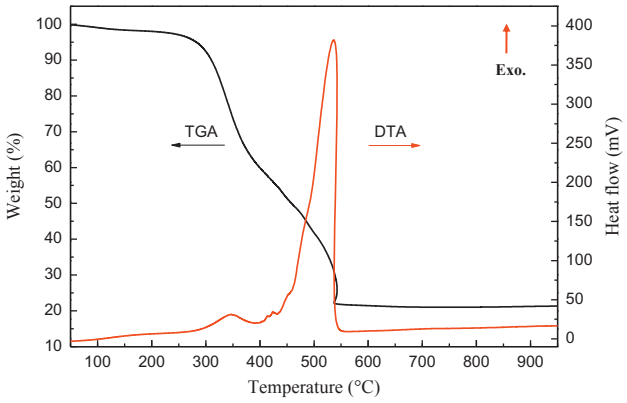

Fig. 3. TG/DTA curves of the precursor resin synthesized using the Pechini method.

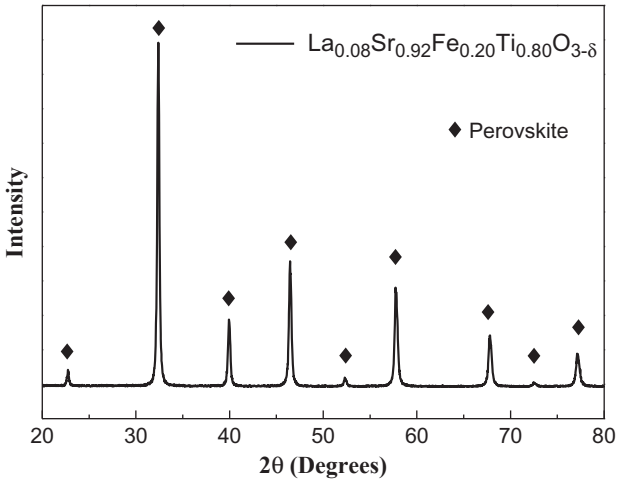

Fig. 4. XRD patterns of $La_{0.08}Sr_{0.92}Fe_{0.20}Ti_{0.80}O_{3-\delta}$ calcined at 800 °C for 5 h in air.

approximately 550 °C, which might be due to the decomposition of organic compounds.

Fig. 4 shows the XRD pattern of La and Fe co-doped $La_{0.08}Sr_{0.92}Fe_{0.20}Ti_{0.80}O_{3-\delta}$ powder synthesized by the Pechini method. A secondary phase-free perovskite-type crystal structure was obtained after calcination at 800 °C for 5 h in air. All XRD peaks were assigned to a single perovskite structure. No other peaks derived from the unreacted raw materials or reacted second phases were observed.

SEM image of the $La_{0.08}Sr_{0.92}Fe_{0.20}Ti_{0.80}O_{3-\delta}$ powder calcined at 800 °C for 5 h by the Pechini method is shown in Fig. 5. The particles were mostly spherical and softly agglomerated. The particle size was estimated to be approximately 100 nm and the BET surface area was 14.7 m^2/g.

Fig. 6 shows the methane conversion rate and hydrogen selectivity over the $La_{0.08}Sr_{0.92}Fe_{0.20}Ti_{0.80}O_{3-\delta}$ catalyst as a function of temperature. The methane oxidation behavior, which strongly depends on the operating temperature, can be divided into three temperature regions. The methane conversion rate increased with increasing temperature from 400 °C to 550 °C, showed a plateau at an intermediate temperature range, 550–750 °C, and increased again at higher temperatures. As

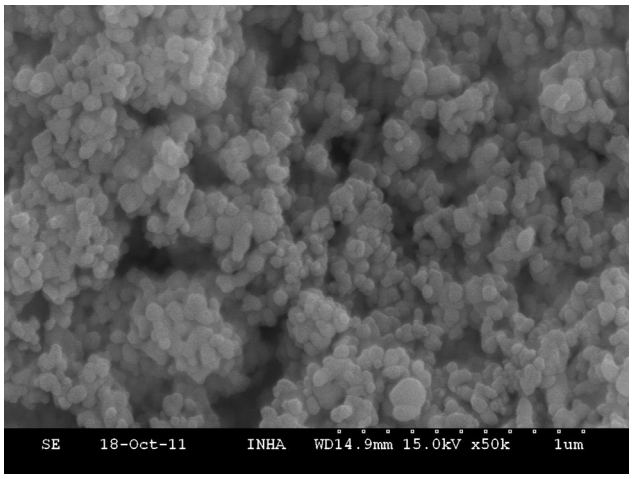

Fig. 5. SEM image of the $La_{0.08}Sr_{0.92}Fe_{0.20}Ti_{0.80}O_{3-\delta}$ powder calcined at 800 °C for 5 h in air.

shown in Fig. 6(b), the hydrogen selectivity was less than 5% up to 650 °C. A drastic increase was observed at 750 °C and higher temperatures. The methane conversion rate and hydrogen selectivity was 52% and 66% at 900 °C, respectively. On the other hand, Tian et al. and Lee et al. have reported that the methane conversion rate of the $SrTiO_3$-based perovskite type catalysts. According to these reports, the methane conversion rate was 16.3∼22.5, depending on the composition of the catalyst or temperature [12,13]. This suggests that the catalytic activity of La and Fe co-doped $La_{0.08}Sr_{0.92}Fe_{0.20}Ti_{0.80}O_{3-\delta}$ powder is much higher than that of the un-doped $SrTiO_3$ powder.

Fig. 7 shows the XPS spectra of the $La_{0.08}Sr_{0.92}Fe_{0.20}Ti_{0.80}O_{3-\delta}$ powder sample and fitting curves for O 1s, Ti 2p and Fe 2p. Titanium species, which are the host ion of the B-site sublattice in perovskite, has a mono-oxidation state, indicating that the titanium ion in the perovskite powder is Ti^{4+}. On the other hand, two peaks overlapped in the Fe 2p spectrum. The deconvoluted XPS curves revealed two peaks at 710.5 eV and 712.6, which were assigned to Fe^{3+} and Fe^{4+}, respectively. This means that the iron in the $La_{0.08}Sr_{0.92}Fe_{0.20}Ti_{0.80}O_{3-\delta}$ perovskite powder has a mixed oxidation state of Fe^{3+} and Fe^{4+}. This result is similar to a previous study [9].

4. Discussion

An analysis of the methane oxidation behavior over a $La_{0.08}Sr_{0.92}Fe_{0.20}Ti_{0.80}O_{3-\delta}$ perovskite catalyst showed that methane conversion occurred differently depending on the temperature range. At low temperatures, the complete oxidation of methane was the most preferential reaction, which can be explained by suprafacial mechanism [14,15] involving oxygen coming from the gas molecules or sitting in the anion vacancies of the oxides [16].

At the intermediate temperatures region, the methane conversion rate did not increase with increasing temperature because oxygen was already consumed by the complete oxidation reaction. As the temperature was increased further, oxygen desorption

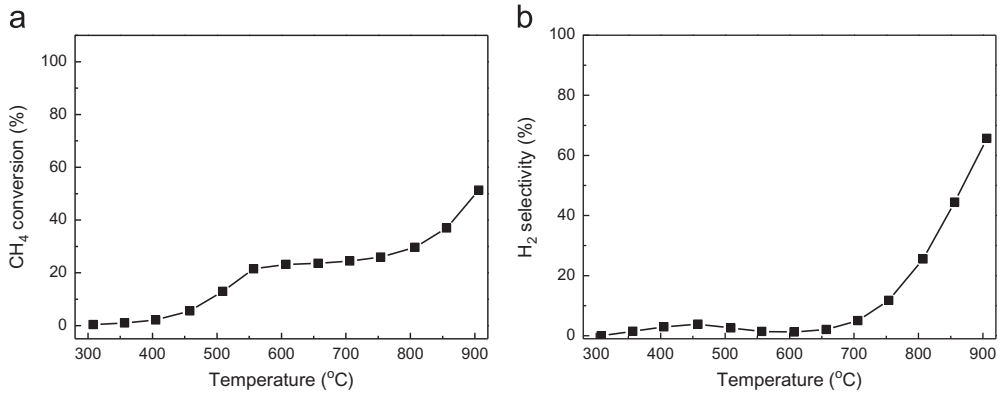

Fig. 6. The methane conversion rate (a) and hydrogen selectivity (b) over the $La_{0.08}Sr_{0.92}Fe_{0.20}Ti_{0.80}O_{3-\delta}$ catalyst sample.

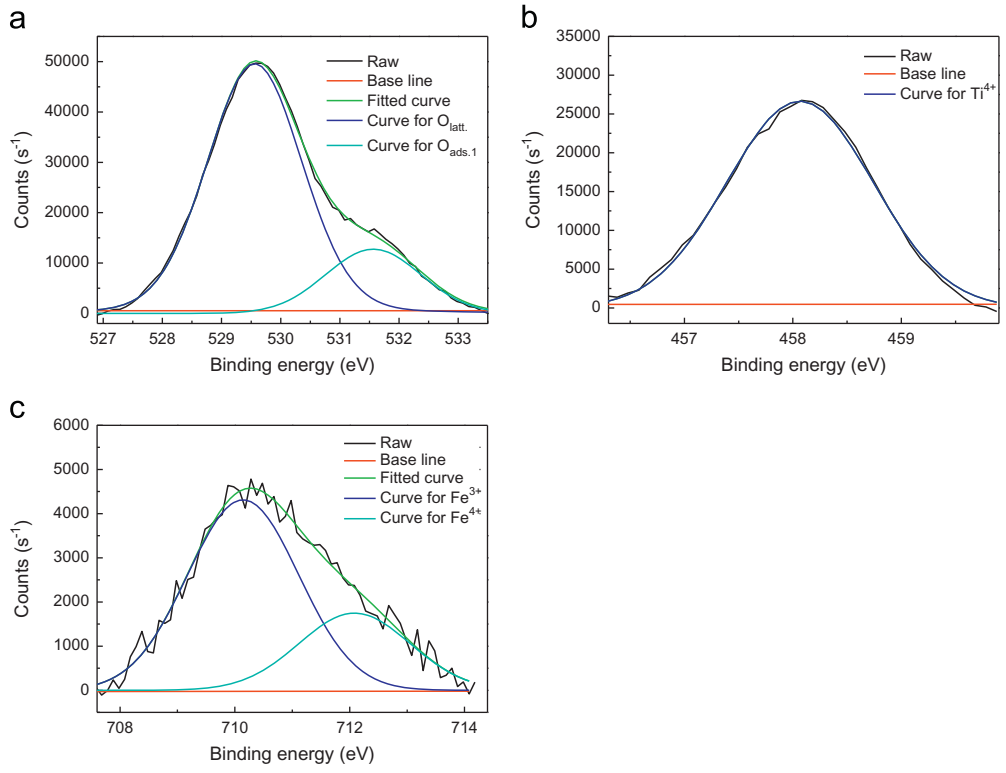

Fig. 7. XPS spectra of the $La_{0.08}Sr_{0.92}Fe_{0.20}Ti_{0.80}O_{3-\delta}$ powder sample for O 1s (a), Ti 2p (b) and Fe 2p (c).

occurred more easily on the catalyst surface than oxygen adsorption because the oxygen molecules are activated by the high thermal kinetic energy. Therefore, the methane conversion rate increased again as a function of temperature, and at the same time, the partial oxidation of methane, which occurs between methane molecules and lattice oxygen of the oxide surface, was observed at high temperatures. The abrupt increase in the hydrogen selectivity might be due to partial oxidation at high temperatures. According to the literature, the lattice oxygen can contribute to the partial oxidation of methane at high temperatures due to an intrafacial mechanism [14,15].

XPS revealed the titanium in the $La_{0.08}Sr_{0.92}Fe_{0.20}Ti_{0.80}O_{3-\delta}$ catalyst to have a mono-oxidation state, whereas iron showed a mixed oxidation state. Accordingly, iron can play an important role as an active site for the high temperature redox mechanism.

5. Conclusions

The La and Fe co-doped single phase perovskite $La_{0.08}Sr_{0.92}Fe_{0.20}Ti_{0.80}O_{3-\delta}$ powder was synthesized using the Pechini method. The methane oxidation behavior over the $La_{0.08}Sr_{0.92}Fe_{0.20}Ti_{0.80}O_{3-\delta}$ catalyst strongly depends on the operating temperature. The partial oxidation of methane by lattice oxygen was predominant at the high temperature region. On the other hand, the complete oxidation of methane due to the adsorbed oxygen molecules was predominant at the low

temperature region. The iron in the catalyst had a mixed oxidation state in the perovskite structure and is believed to be an active site for the high temperature redox mechanism.

Acknowledgments

This research was supported by a grant from the Fundamental R&D Program for Core Technology of Materials funded by the Ministry of Knowledge Economy, Republic of Korea. A part of this work was supported by the National Research Foundation of Korea (NRF) grant funded by the Korea government (MEST) (No. 2010-0010744).

References

[1] B.C.H. Steele, Running on natural gas, Nature 400 (1999) 619–621.
[2] A. Atkinson, S. Barnett, R.J. Gorte, J.T.S. Irvine, A.J. McEvoy, M. Mogensen, S.C. Singhal, J. Vohs, Advanced anodes for high-temperature fuel cells, Nature Materials 3 (2004) 17–27.
[3] C.H. Bartholomew, Carbon deposition in steam reforming and methanation, Catalysis Reviews—Science and Engineering 24 (1982) 67–112.
[4] T. Takeguchi, Y. Kani, T. Yano, R. Kikuchi, K. Eguchi, K. Tsujimoto, Y. Uchida, A. Ueno, K. Omoshiki, M. Aizawa, Study on steam reforming of CH_4 and C_2 hydrocarbons and carbon deposition on Ni–YSZ cermets, Journal of Power Sources 112 (2002) 588–595.
[5] K. Sasaki, Y. Teraoka, Equilibria in fuel cell gases: I. equilibrium compositions and reforming conditions, Journal of the Electrochemical Society 150 (2003) A878–A884.
[6] C.D. Savaniu, J.T.S. Irvine, La-doped $SrTiO_3$ as anode material for IT-SOFC, Solid State Ionics 192 (2011) 491–493.
[7] K.B. Yoo, G.M. Choi, Performance of La-doped strontium titanate (LST) anode on $LaGaO_3$-based SOFC, Solid State Ionics 180 (2009) 867–871.
[8] M.R. Pillai, I. Kim, D.M. Bierschenk, S.A. Barnett, Fuel-flexible operation of a solid oxide fuel cell with $Sr_{0.8}La_{0.2}TiO_3$ support, Journal of Power Sources 185 (2008) 1086–1093.
[9] M. Ghaffari, M. Shannon, H. Hui, O.K. Tan, A. Irannejad, Preparation, surface state and band structure studies of $SrTi_{(1-x)}Fe_{(x)}O_{(3-\delta)}$ ($x=0$–1) perovskite-type nano structure by X-ray and ultraviolet photoelectron spectroscopy, Surface Science 606 (2012) 670–677.
[10] H.M. Zhang, Y. Teraoka, N. Yamazoe, Preparation of perovskite-type oxides with large surface area by citrate process, Chemistry Letters 16 (1987) 665–668.
[11] C. Mao, X. Dong, T. Zeng, G. Wang, S. Chen, Formation and control of mechanism for the preparation of ultra-fine barium strontium titanate powders by the citrate precursor method, Materials Research Bulletin 42 (2007) 1602–1610.
[12] T. Tian, W. Wang, M. Zhan, C. Chen, Catalytic partial oxidation of methane over $SrTiO_3$ with oxygen-permeable membrane reactor, Catalysis Communications 11 (2010) 624–628.
[13] M. Lee, J. Jun, J. Jung, Y. Kim, S. Lee, Catalytic activities of perovskite-type $LaBO_3$ (B=Fe, Co, Ni) oxides for partial oxidation of methane, Bulletin of the Korean Chemical Society 26 (2005) 1591–1596.
[14] N. Yamazoe, Y. Teraoka, Oxidation catalysis of perovskites—relationships to bulk structure and composition (valency, defect, etc.), Catalysis Today 8 (1990) 175–199.
[15] J.L.G. Fierro, Structure and composition of perovskite surface in relation to adsorption and catalytic properties, Catalysis Today 8 (1990) 153–174.
[16] K.S. Chan, J. Ma, S. Jaenicke, G.K. Chuah, J.Y. Lee, Catalytic carbon monoxide oxidation over strontium, cerium and copper-substituted lanthanum manganates and cobaltates, Applied Catalysis A: General 107 (1994) 201–227.